Macromolecules

pubs.acs.org/Macromolecules Article

Elemental Selenium-Derived Poly(sulfide selenide)s: A Platform of Photodegradable and Electrochemical Responsive Polymers

Tian-Jun Yue,[§] Xiang-Yu Fu,[§] Ji Zhang, Yong-Gui Zhou, Wei-Min Ren,* and Xiao-Bing Lu

Cite This: *Macromolecules* 2024, 57, 1319−1327

Read Online

ACCESS | Metrics & More | Article Recommendations | Supporting Information

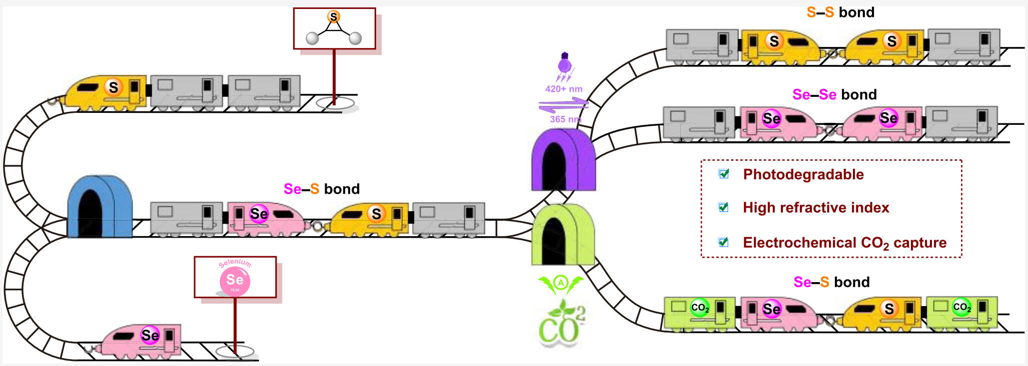

ABSTRACT: Selenium-containing polymers have numerous attractive properties, such as light response behaviors, biocompatibilities, and heavy-metal-ion adhesive ability. However, the lack of efficient strategies for constructing selenium-containing polymers limits their development. Herein, a facile but efficient strategy is proposed for synthesizing poly(sulfide selenide)s directly from elemental selenium and episulfides in the presence of an organocatalyst system. This strategy affords diverse poly(sulfide selenide)s with high sulfide−selenide linkage selectivity (>99%). The mechanism exploration reveals that the sulfide−selenide linkage selectivity is affected by the nucleophilicity of the organic bases: the organic base with high nucleophilicity leads to the high sulfide−selenide linkage selectivity. Notably, the poly(sulfide selenide)s exhibit excellent photodegradable nature. Furthermore, the excellent electrochemical properties of these poly(sulfide selenide)s enable their application in electrochemical CO_2 capture. The high monomer compatibility of this method leads to a series of poly(sulfide selenide)s with diverse structures and thus various thermal and optical performances.

INTRODUCTION

The interest in selenium research has progressed in recent decades due to the excellent features of elemental selenium, including dramatic electrochemistry properties, biological values, and extensive pharmaceutical applications.[1−5] Hence, selenium is widely studied in materials science, biological sciences, and synthetic chemistry. For example, the Se−Li battery is a promising candidate for next-generation high-energy-density batteries because of its excellent performance, high theoretical volume energy density, and high controllability in an electrochemical cell.[6,7] In addition, elemental selenium can stimulate the organogenesis and growth of the root system and improve antiviral activity in animals.[8,9] New and promising drugs and pesticides are also achievable when the two sulfur atoms of the dithiophosphinates are replaced by Se atoms.[10] Selenium also exhibits its advantages in a polymeric material by promoting electrical conductivity, optical performance, and adhesive ability to heavy metal ions of the polymers.[11−17] For instance, poly(selenophene-perylene diimide)s can be used as the charge acceptors for polymer solar cells owing to their high hole and charge-carrier mobilities.[11] Poly(oxaselenolane)s and selenium-containing polythioesters possess a high refractive index,[12,13] while polyselenoureas can selectively enrich heavy metal ions.[14] In this context, achieving the applicability of selenium chemistry in polymer science is of great importance, for which developing an efficient synthetic methodology to construct selenium-containing chemical bonds is essential.

Polymers containing sulfur−selenium (S−Se) bonds are gaining significant attention due to their dynamic characteristic.[18−20] Dynamic covalent bonds (DCBs) are a category of chemical bonds that undergo reversible cleavage and formation autonomously or in response to stimulation.[21,22] Because of these intrinsic characteristics, polymers containing DCBs have remarkable properties, such as self-healing, shape memory,

Received: August 15, 2023
Revised: January 6, 2024
Accepted: January 12, 2024
Published: February 2, 2024

https://doi.org/10.1021/acs.macromol.3c01628
Macromolecules 2024, 57, 1319−1327

Scheme 1. Strategies for Constructing Polymers Containing Sulfide−Selenide (S−Se) Bonds

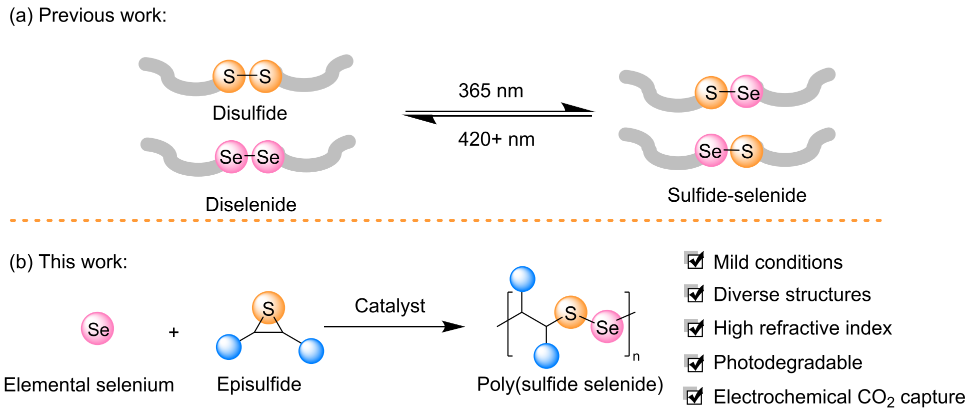

Table 1. Yields of the Copolymerization of Elemental Selenium and Propylene Sulfide[a]

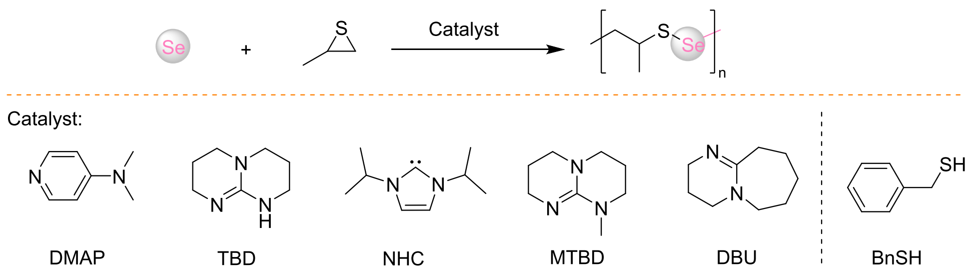

entry	catalyst	MT/[Se]/catalyst/BnSH[b]	temp. (°C)	time (h)	conv.[c] (%)	linkage selectivity[d] (%)	M_n[e] (kg mol^{-1})	$Đ$[e] (M_w/M_n)
1		800/800/--/10	25	48	n.r.[f]	[g]	[g]	[g]
2	DMAP	800/800/1/10	25	2	26	76	4.2	1.80
3	TBD	800/800/1/10	25	2	>99	94	2.5	1.37
4	NHC	800/800/1/10	25	24	36	71	0.7	1.63
5	MTBD	800/800/1/10	25	0.6	>99	97	3.1	1.71
6	DBU	800/800/1/10	25	0.4	>99	99	8.7	1.32
7	DBU	800/800/1/10	0	3	>99	94	7.9	1.29
8	DBU	800/800/1/10	50	0.2	>99	>99	5.9	1.57
9[h]	DBU	800/400/1/10	25	0.2	>99	56	7.3	1.46
10	DBU	500/1200/1/10	25	1.0	>99	63	0.9	1.34
11	DBU	1600/1600/1/10	25	0.8	>99	99	9.3	1.45
12	DBU	4000/4000/1/10	25	2.0	>99	99	23.4	1.25
13	DBU	8000/8000/1/10	25	3.0	>99	99	26.2	1.31
14	DBU	800/800/1/1	25	1	>99	>99	16.2	1.33
15	DBU	800/800/1/5	25	0.8	>99	>99	11.1	1.37
16	DBU	800/800/1/20	25	0.2	>99	97	1.1	1.32
17	DBU	800/800/1/50	25	0.2	>99	98	1.4	1.29
18	DBU	800/800/1/100	25	0.2	>99	97	0.8	1.25

[a]All the reactions were performed in 2-methylthriiane (MT, 20 mmol) containing organic bases (0.025 mmol) and benzyl mercaptan (BnSH, 0.25 mmol, unless noted) in the presence of 1,4-dioxane ($V_{1,4\text{-dioxane}}/V_{MT}$ = 1:1). No thioether linkages were observed from the ^{1}H NMR spectra of the copolymers except for entry 9. [b]The ratio mentioned in this manuscript refers to the molar ratio of thiirane to selenium atoms. [c]Conversion of MT, determined by ^{1}H NMR spectroscopy. [d]Linkage selectivity is the S−Se linkage, which is calculated from the ^{1}H NMR spectrum as S−Se linkage = $A_{3.38-3.60}/(A_{3.38-3.60} + A_{3.60-3.88}) \times 100\%$. [e]Number-average molecular weight of the polymer, determined by gel permeation chromatography in $CHCl_3$ and calibrated with polystyrene standards. [f]n.r. indicates that copolymerization did not proceeded. [g]Not detected. [h]S−Se linkage selectivity remained >99% before elemental selenium was fully consumed.

adaptability, stress relaxation, and responsiveness.[23−29] As a light-responsive DCB, the asymmetric structure of the S−Se bond allows the polymers to undergo wavelength-controlled assembly in morphology and chemical compositions.[18,19] In chalcogenides, sulfur and selenium can easily form dynamic S−S and Se−Se bonds. The bond energy of S−S is 240 kJ mol^{-1} (cleavage under the irradiation of 365 nm ultraviolet−visible (UV−vis) light), while that of Se−Se is 172 kJ mol^{-1} (cleavage under the irradiation of 450 nm visible light), suggesting that the S−S bond is more stable than the Se−Se bond.[30] The treatment of an S−S and Se−Se mixture with UV−vis light at a wavelength of 365 nm leads to the formation of S−Se, whose bond energy is 207 kJ mol^{-1}, which can then be cleaved by irradiating under the 410 nm-UV−vis light.[31] Hence, when the polymers containing S−Se bonds are irradiated under visible light, a greater number of S−S bonds are generated as both S−Se and Se−Se bonds are cleaved, which triggers the morphology and chemical composition assembly and causes

https://doi.org/10.1021/acs.macromol.3c01628
Macromolecules 2024, 57, 1319−1327

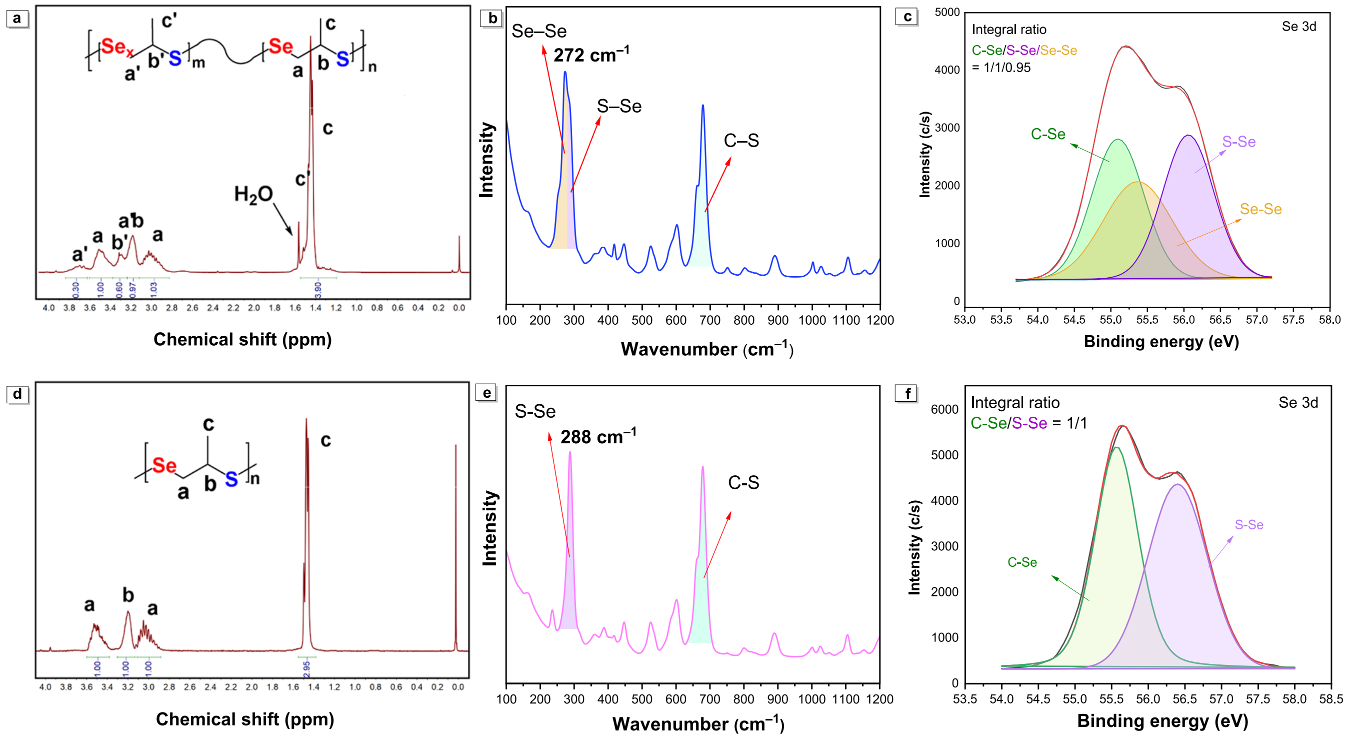

Figure 1. Characterizations of the obtained Se/MT copolymers: (a) ^{1}H NMR, (b) Raman, and (c) X-ray photoelectron spectra of the copolymers obtained using DMAP and BnSH; (d) ^{1}H NMR, (e) Raman, and (f) X-ray photoelectron spectra of the copolymers obtained using DBU and BnSH.

variations in polymer properties. For example, the assembling behavior of polymer vesicles can be regulated using light at different wavelengths by introducing the S−Se DCB.[18]

Currently, the common method for directly constructing the S−Se bond mainly includes the metathesis of S−S and Se−Se bonds under the irradiation of 365 nm-UV−vis light (Scheme 1a).[31] However, the S−S and Se−Se bonds coexist in the system due to the reversible nature of the metathesis reaction, which is a drawback of this method. Thus, facile and efficient strategies for constructing S−Se bonds are essential to further develop polymers containing S−Se DCBs. Herein, we propose the construction of S−Se bonds by copolymerizing elemental selenium with episulfides in a controlled manner (Scheme 1b). This strategy shows good episulfide compatibility, affording a series of poly(sulfide selenide)s with diverse structures. Moreover, the photodegradation behavior was investigated by irradiating poly(sulfide selenide)s with 365 nm-UV−vis light. The newly generated S−S and Se−Se segments, along with the residual S−Se segments, suggest that the wavelength-controlled morphology and chemical composition modification are feasible. In addition, the electrochemical capture of CO_2 with poly(sulfide selenide)s is accessible using a sulfide/selenide−thiocarbonate/selenocarbonate redox cycle.

■ RESULTS AND DISCUSSION

Se/2-Methylthriiane (MT) Copolymerization. Elemental selenium can reportedly be incorporated into organoselenium compounds via the nucleophilic attack.[32−34] Therefore, the construction of S−Se would be feasible when thiolate anion species (R−S^{-}), a strong nucleophile, is generated in situ, followed by the nucleophilic attack on elemental selenium. Recent research revealed that the ring-opening of episulfides is efficient in producing thiolate anions when copolymerizing with carbon disulfide, cyclic thioanhydride, isothiocyanates, and elemental sulfur to produce the corresponding copolymers. This is because episulfides easily undergo ring-opening in the presence of nucleophiles, such as organic bases and even organic ammonium salts.[35−38] In this context, we propose the copolymerization of elemental selenium and episulfides with a binary catalyst system consisting of organic bases and benzyl mercaptan (BnSH). Initially, the copolymerization of elemental selenium with propylene sulfide (also known as 2-methylthriiane; MT) was performed in the presence of only BnSH. No MT conversion was detected after the copolymerization proceeded for 48 h (Table 1, entry 1). Subsequently, a series of organic bases were screened for achieving copolymerization. When 4-dimethylaminopyridine (DMAP) was used, an MT conversion of 26% was observed after the reaction proceeded for 2 h. The molecular weight (M_n) of the obtained copolymer was 4.2 kg mol^{-1} with a molecular weight dispersity ($Đ$) of 1.80 (entry 2). ^{1}H NMR analysis of the obtained copolymer showed two arrays of peaks, indicating a mixed linkage structure (Figure 1a). Further characterization of the copolymer by Raman spectroscopy (Figure 1b) and X-ray photoelectron spectroscopy (XPS; Figure 1c) revealed that the copolymer contains S−Se and S−Se$_x$ (x > 1) segments. Characterization of the resultant copolymer with ^{77}Se NMR spectroscopy further indicated the complicate structure characteristic of this copolymer, wherein a set of peaks at δ 310.6−332.4, 455.9, 482.7, and 589.2−608.3 ppm were observed from the ^{77}Se NMR spectrum (Figure S1a). Considering this, the peak at δ 3.125 ppm in the ^{1}H NMR spectrum can be ascribed to the methine of the S−Se linkage, while that at δ 3.265 ppm can be ascribed to the S−Se$_x$ (x > 1) linkage. Therefore, the S−Se linkage selectivity of the copolymer obtained from DMAP-mediated copolymerization

https://doi.org/10.1021/acs.macromol.3c01628
Macromolecules 2024, 57, 1319−1327

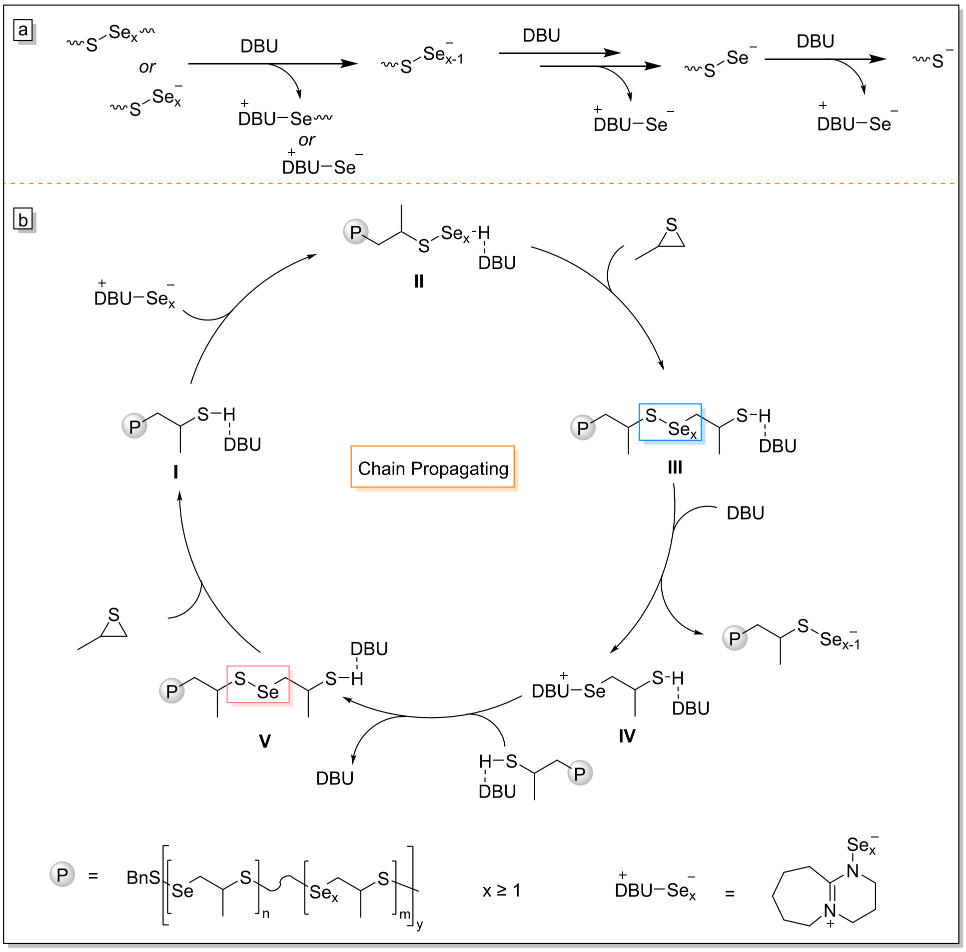

Figure 2. Proposed mechanism for the copolymerization of Se and MT: (a) transformation of S−Se_x linkage into S−Se linkage and (b) chain propagation process.

can be calculated to be 76%. Other organic bases, such as 1,5,7-triazabicyclo[4.4.0]dec-5-ene (TBD), N-heterocyclic carbene (NHC), 7-methyl-1,5,7-triazabicyclo[4.4.0]dec-5-ene (MTBD), and 1,8-diazabicyclo[5.4.0]undec-7-ene (DBU), could also mediate Se/MT copolymerization in different efficiency and S−Se linkage selectivity (entries 3−6). Notably, only one array of peaks with the ratio of 1:1:1:3 was observed in the ^{1}H NMR spectrum of the resulted copolymer when DBU was used (Figure 1d). Correspondingly, the heterogeneous reaction mixture gradually transformed into a dark brown homogeneous solution and then into a brown solution (Figure S2). In addition, almost no peak representing the Se−Se_x bond was observed in the Raman spectrum (Figure 1e), suggesting that DBU could mediate Se/MT copolymerization with high S−Se selectivity (99%). The ^{77}Se NMR spectra of this copolymer indicated its high S−Se selectivity nature, as only one group of peaks at δ 310.6−332.4 ppm was observed from the ^{77}Se NMR spectra of this copolymer (Figure S1b). This is further supported by the XPS result (Figure 1f) and ^{1}H−^{1}H COSY NMR analysis (Figure S3). Hence, DBU was selected as a catalyst for the subsequent investigation. Regretfully, the acquirement of detail structure information with mass spectroscopy, including the matrix-assisted laser desorption ionization-time-of-flight mass spectrometry (MALDI-TOF-MS) and electrospray ionization mass spectrometry (ESI-MS), was unavailable due to the weak bond strength nature of the S−Se bond, which is easily broken under the ESI-MS conditions (Figure S4).

The Se/MT copolymerization was further investigated by exploring the influence on efficiency and selectivity produced by the reaction temperature. Lowering the temperature to 0 °C caused a decrease in copolymerization efficiency and a slight loss in the S−Se linkage selectivity, affording a copolymer with M_n of 7.9 kg mol^{-1} and $Đ$ of 1.29 (entry 7). Elevating the reaction temperature to 50 °C accelerated copolymerization, while the S−Se linkage selectivity remained >99%, affording a copolymer with M_n of 5.9 kg mol^{-1} and $Đ$ of 1.57 (entry 8). The MT transformation efficiency was higher when the elemental selenium loading was reduced, as the MT was fully consumed in 0.2 h, providing a copolymer with a lower S−Se linkage selectivity of 56% of the final copolymer. Notably, the S−Se linkage selectivity remained >99% before the elemental selenium was fully consumed (entry 9). In contrast to the case of MT excess, copolymerization decelerated as the elemental selenium loading increased, affording a copolymer with a decreased S−Se linkage selectivity of 63% (entry 10). In addition, the Se/MT copolymerization could proceed in higher feed ratios from 1600/200/1/10 to 4000/500/1/10 and to 8000/1000/1/10, yielding the corresponding poly(sulfide selenide)s with increased M_ns (from 9.3 to 23.4 and 26.2 kg mol^{-1}, respectively) and without losing the S−Se linkage selectivity (entries 11−13). Additionally, poly(sulfide selenide)s with

https://doi.org/10.1021/acs.macromol.3c01628
Macromolecules 2024, 57, 1319−1327

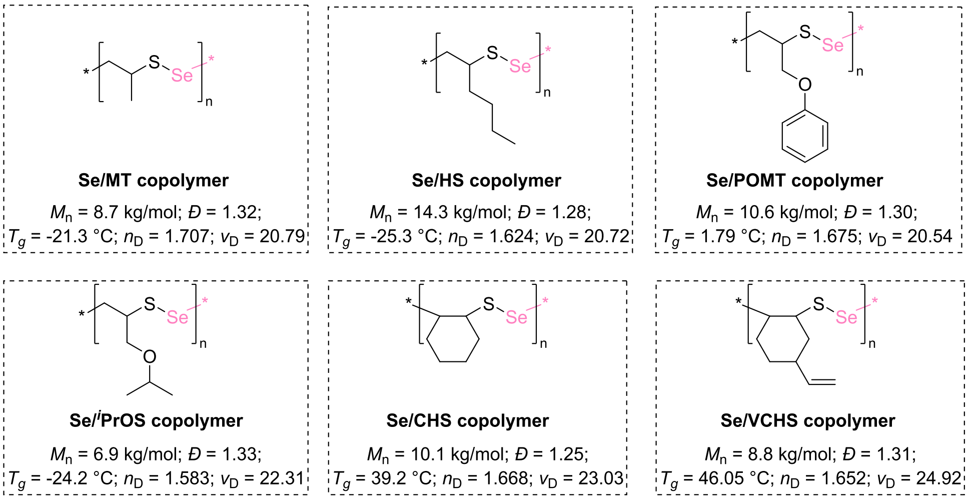

Figure 3. Synthesis of various poly(sulfide selenide)s.

higher M_ns of 16.2 and 11.1 kg mol^{-1} were obtained when 1 and 5 equiv of BnSH-to-DBU were added, respectively (entries 14 and 15). The increase in BnSH also facilitated copolymerization, yielding copolymers with lower M_ns and S−Se linkage selectivity (entries 16−18). Besides, other thiols, like ^{n}butanethiol, allyl mercaptan ethanedithiol, are also capable for the copolymerization in high efficiency without decreasing the S−Se linkage selectivity (Table S1).

Mechanism Exploration of Se/MT Copolymerization. Our previous work, in which the copolymerization of elemental sulfur with episulfides was reported for synthesizing polydisulfides, disclosed that the organic ammonium salts with a non-nucleophilic anion, like [PPN]SbF_6, are essential for obtaining polydisulfides with high linkage selectivity.[38] However, for the copolymerization of Se/MT, the non-nucleophilic organic ammonium salts are inessential. To shed more light on how the copolymerization proceeded, the process was monitored by means of NMR with intermittent sampling experiments. The peaks representing the S−Se linkages were observed after the copolymerization proceeded for 4 min, and the intensity of these peaks increased with the decrease of MT, accompanied by the color change of the reaction mixture form dark to yellow (Figure S5). Simultaneously, the signals representing S−Se_x linkages were also detected and subsequently disappeared as MT fully converted. Similarly, tracing the copolymerization with ^{77}Se NMR spectra also indicated that the Se−Se_x linkages first formed and then converted into S−Se linkages with the copolymerization proceeding (Figure S6). These results indicate the S−Se_x linkage transformed into the S−Se linkage with the consumption of MT, implying that the cleavage of the S−Se bond in the S−Se_x linkages happened in the course of the copolymerization. In addition, DBU was proposed for acting as the nucleophile for breaking the S−Se bond in the S−Se_x linkages (Figure 2a). In this context, the mechanism for the chain propagating process of the Se/MT copolymerization was proposed as follows (Figure 2b): intermediate **I** (thiolate, generated from the ring-opening of a MT) nucleophilic attacks at the DBU^+−Se_x^- species to yield intermediate **II**, which is followed by the insertion of the next MT, thus forming the S−Se_x linkage (intermediate **III**). Then, the nucleophilic attack of DBU at the Se−Se in the S−Se_{x-1} linkage (Figure 2a) produces intermediate **IV** and living polymer chain species, which participates in the chain propagation as intermediate **II**. Subsequently, the exchange of thiolate and DBU in intermediate **IV** yields the S−Se linkage (intermediate **V**) with release of a DBU. The insertion of another MT leads to the finish of one chain propagating cycle. With regard to this mechanism, the nucleophilic attack from the organic base is the key to the conversion of the S−Se_x linkage into the S−Se linkage, which is largely affected by the nucleophilicity of the organic bases. The organic bases with strong nucleophilicity, like TBD, MTBD, and DBU, led to the high S−Se linkage selectivity (entries 3, 5, and 6, Table 1). However, the organic bases with weak nucleophilicity, including DMAP and NHC, resulted in the low S−Se linkage selectivity (entries 2 and 4).

Synthesis of Various Poly(sulfide selenide)s. To obtain poly(sulfide selenide)s with diverse structures, the copolymerization of elemental selenium with various episulfides was performed with the feed ratio of [Se]/episulfides/DBU/BnSH = 800:800:1:10 in the presence of toluene ($V_{toluene}/V_{episulfide}$ = 1:1) at 25 °C (Figure 3). The conversion of all episulfides reached over 99% in 1 h, providing the corresponding poly(sulfide selenide)s with the S−Se linkage selectivity >99% (Figures S7−S12). These results suggest that this strategy possesses good compatibility with various episulfides. The thermal properties of these poly(sulfide selenide)s were characterized by using differential scanning calorimetry and thermogravimetric analysis. The poly(sulfide selenide)s were observed to be amorphous with their T_gs ranging from −34 to 46 °C, suggesting a "soft" nature of these polymers and their suitability for application in the self-healing materials (Figures S13−S19). Furthermore, the 5% weight loss decomposition temperature of these poly(sulfide selenide)s ranges from 157.2 to 235.7 °C (Figures S20−S26). Notably, these copolymers possess a high refractive index ranging from 1.562 to 1.707, which was determined by using an elliptical polarization spectrometer (Figure S27). The high refractive indexes of these polymers can be attributed to the high S−Se content, due to the high molar refraction of chalcogenides. The corresponding Abbe number of these copolymers was calculated to be over 20 (Table S2).

Photodegradation Behavior Study of the Poly(sulfide selenide). The response of polymers containing the S−Se bond to light stimulation is achieved through structural reassembly, thus triggering the performance reassembly.[18]

https://doi.org/10.1021/acs.macromol.3c01628
Macromolecules 2024, 57, 1319−1327

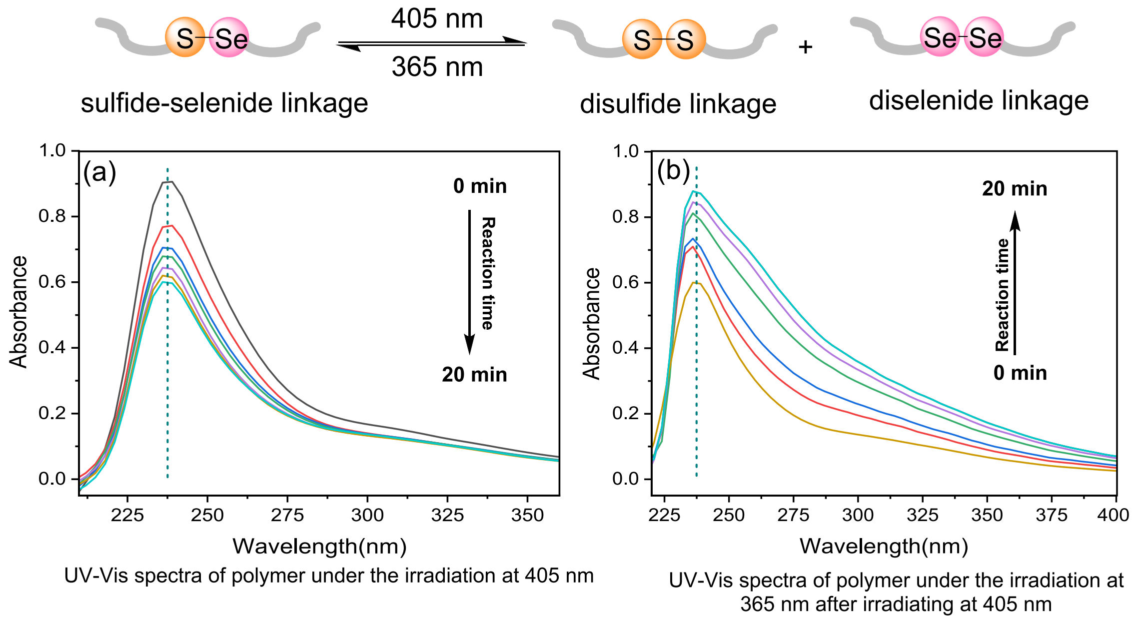

Figure 4. Variation of UV−vis absorbance of the Se/MT copolymer with irradiating time at different wavelengths: (a) 405 and (b) 365 nm after being irradiated at 405 nm.

The photodegradation behaviors of poly(sulfide selenide)s were also explored in this study by investigating the transformation of the S−Se bond between the S−S and Se−Se bonds under the irradiation of UV−vis light at 405 and 365 nm, respectively. The maximum UV−vis absorbance wavelength of the S−S and Se−Se bonds was confirmed with reference to 1,2-dimethyldisulfane (CH_3SSCH_3) and 1,2-dimethyldiselane ($CH_3SeSeCH_3$) due to their structural similarity to repeat the Se/MT copolymer unit. The maximum UV−vis absorbance wavelength of the S−S and Se−Se bonds was found to be 255 and 315 nm, respectively (Figure S28a,b), while that of the S−Se bond in methyl(methylselanyl)sulfane (CH_3SSeCH_3) was 248 nm (Figure S29). Subsequently, the photodegradation behavior of the Se/MT copolymer, which was coated on a quartz glass slide, was explored by using a UV−vis spectrophotometer. An absorbance peak at λ = 238 nm was detected, which is attributed to the maximum absorbance of the S−Se bond in the Se/MT copolymer.[39] However, the absorbance decreased with the irradiation time when the Se/MT copolymer was irradiated under 405 nm-UV−vis light, suggesting the cleavage of the S−Se bonds (Figure 4a). Accordingly, the M_n of the Se/MT copolymer decreased from 3.2 kg mol^{-1} ($Đ$ = 1.35) to 1.7 kg mol^{-1} ($Đ$ = 1.52) (Figure S30). Furthermore, when the previously irradiated Se/MT copolymer was treated with 365 nm-UV−vis light, the absorbance increased with the irradiating time, implying that the S−Se bonds reformed via the reassembling of the cleaved −C−S$^\bullet$ and −C−Se$^\bullet$ fragments (Figure 4b). Notably, a similar situation, in which the absorbance at the maximum absorbance wavelength decreased when irradiated under 405 nm-UV−vis light and subsequently increased when irradiated under 365 nm-UV−vis light, was observed in the Se/MT copolymer-containing dichloromethane solution (0.028 mg mL^{-1}) (Figure S31). To gain more information on the photodegradation behavior of the poly(sulfide selenide), the copolymer obtained from the copolymerization of Se with 2-(phenoxymethyl)thiirane (POMT) was employed for the photodegradation behavior study. The fragments generated from the UV−vis light (λ = 405 nm)-irradiated Se/POMT copolymer were analyzed using XPS, ^{1}H NMR spectroscopy, and electrospray ionization mass spectrometry (ESI-MS). XPS analysis revealed that more C−Se was formed as the ratio of C−Se to S−Se bonds increased from 1:1 to 1.3:1 (Figure S32). This can be attributed to the formation of Se−Se bonds after the polymer was irradiated under UV−vis light. Moreover, the peaks in the ^{1}H NMR spectrum of the copolymer became rough with the newly appeared peaks after being irradiated under the UV−vis light at a wavelength of 405 nm (Figure S33). The analysis of the purified low-molecular-weight Se/POMT copolymer fragments, obtained through column chromatography, by ^{1}H NMR spectroscopy showed more specifically split peaks of the fragments (Figure S34). The purified fragments were further characterized as the S−S, S−Se, and Se−Se coexisting fragments since a peak with m/z = 844.7879 was observed in the ESI-MS spectrum (Figure S35).[40] These results suggest that the photodegradation of poly(sulfide selenide)s yields the products with the assembly structure from the generated species, indicating their potential application in photostimulated and responsive smart materials.

Electrochemical Capture of CO_2 with Poly(sulfide selenide)s. The electrochemical cycle for capturing and releasing CO_2 has gained increasing attention in recent years.[41−44] A successful electrochemical CO_2 capture is achieved when the electrochemical process allows the in situ generation of nucleophiles, which capture CO_2 through a nucleophilic interaction. For poly(sulfide selenide)s, a thiolate and selenolate with strong nucleophilicity are readily feasible through an electrochemical reduction process, as the valency of sulfur and selenium in the poly(sulfide selenide)s is reduced from −1 to −2, thus allowing the CO_2-capturing process. Accordingly, cyclic voltammetry of the Se/MT copolymer was conducted in mixed solvent of dimethylformamide and toluene in the presence of tetrabutylammonium tetrafluoroborate at a concentration of 20 mM. The cyclic voltammogram of poly(sulfide selenide)s revealed that the corresponding thiolate and selenolate species were generated as two peaks appeared at

https://doi.org/10.1021/acs.macromol.3c01628
Macromolecules 2024, 57, 1319−1327

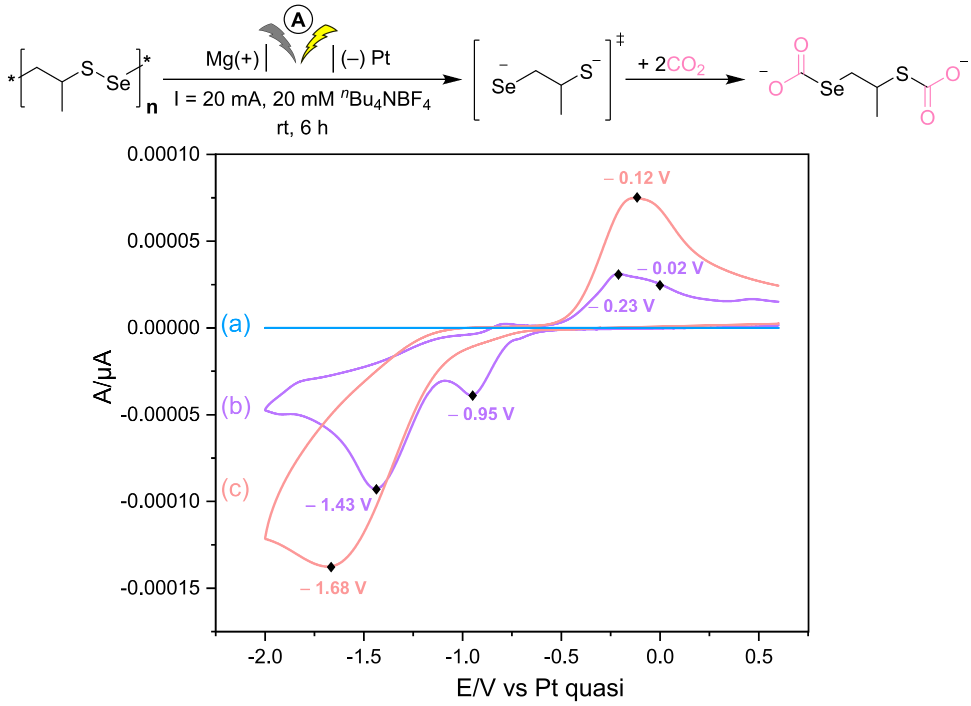

Figure 5. Cyclic voltammetry of poly(sulfide selenide)s under different conditions: (A) only electrolyte solution; (B) 20 mM Se/MT copolymer in the electrolyte solution; (C) 20 mM Se/MT copolymer in the electrolyte solution and in the presence of CO_2. Conditions: electrolyte solution:tetrabutylammonium tetrafluoroborate dissolved in a mixed solution of dimethylformamide and toluene (V_{DMF}/V_{tol} = 4:1); working, glassy carbon electrode; reference and counter, Pt electrode; scan rate, 10 mV s^{-1}.

−0.95 and −1.43 V, respectively (Figure 5a,b). The subsequent positive-going scan showed the appearance of two oxidation peaks at −0.23 and −0.02 V, indicating the regeneration of S−Se bonds. The reduction peak shifted to −1.68 V in the presence of CO_2 (Figure 5c). The reaction mixture was then examined by Fourier transform infrared spectroscopy (FT-IR) after being treated with iodomethane. Two peaks at wavenumbers (σ) of 1732 and 1654 cm^{-1}, which can be attributed to the $\nu_{C=O}$ absorption of monothiocarbonate (−SCOO⁻) and monoselenocarbonate (−SeCOO⁻), respectively, were observed (Figure S36). The peaks at δ = 168.7 and 171.0 ppm were assigned to −SCOO− and −SeCOO−, respectively, as analyzed by ^{13}C NMR of the further purified product (Figure S37). These results indicate the formation of monothiocarbonate and monoselenocarbonate species; that is, the electrochemical CO_2 capture is accessible with poly(sulfide selenide)s. Additionally, an oxidation peak was observed at −0.12 V, which is caused by the thiocarbonate and selenocarbonate species. A similar result was observed in the case of electrochemical CO_2 capture using a disulfide−thiocarbonate redox cycle.[44] Furthermore, this electrochemical CO_2 capture−release process can be repeated 3 times as monitored by the in situ FT-IR (Figures S38−S39). Hence, the electrochemical cycle that enables the capture and release of CO_2 is possible using poly(sulfide selenide)s.

■ CONCLUSIONS

In summary, a poly(sulfide selenide) synthetic platform, which allows the production of various poly(sulfide selenide)s with well-defined structures, was constructed through organobase-mediated copolymerization using elemental selenium and episulfides. Notably, these poly(sulfide selenide)s are photo-degradable and can respond to UV−vis light stimulation through the structural assembly. Moreover, the obtained poly(sulfide selenide)s could be used for electrochemical CO_2 capture via the reversible breaking and formation sulfide−selenide bonds. Currently, the research on synthesizing self-healable poly(sulfide selenide)s-based materials with enhanced properties is ongoing.

■ ASSOCIATED CONTENT

Supporting Information

The Supporting Information is available free of charge at https://pubs.acs.org/doi/10.1021/acs.macromol.3c01628.

General experimental procedures and characterizations of copolymers (PDF)

■ AUTHOR INFORMATION

Corresponding Author

Wei-Min Ren − *State Key Laboratory of Fine Chemicals, Frontiers Science Center for Smart Materials, Dalian University of Technology, Dalian 116024, China;* orcid.org/0000-0003-4425-1453; Email: wmren@dlut.edu.cn

Authors

Tian-Jun Yue − *State Key Laboratory of Fine Chemicals, Frontiers Science Center for Smart Materials, Dalian University of Technology, Dalian 116024, China;* orcid.org/0000-0002-1579-5585

Xiang-Yu Fu − *State Key Laboratory of Fine Chemicals, Frontiers Science Center for Smart Materials, Dalian University of Technology, Dalian 116024, China*

Ji Zhang − *State Key Laboratory of Fine Chemicals, Frontiers Science Center for Smart Materials, Dalian University of Technology, Dalian 116024, China*

https://doi.org/10.1021/acs.macromol.3c01628
Macromolecules 2024, 57, 1319−1327

Yong-Gui Zhou − *Zhang Dayu School of Chemistry, Dalian University of Technology, Dalian 116024, China;* orcid.org/0000-0002-3321-5521

Xiao-Bing Lu − *State Key Laboratory of Fine Chemicals, Frontiers Science Center for Smart Materials, Dalian University of Technology, Dalian 116024, China;* orcid.org/0000-0001-7030-6724

Complete contact information is available at: https://pubs.acs.org/10.1021/acs.macromol.3c01628

Author Contributions

§T.-J.Y. and X.-Y.F. contributed equally to this work.

Notes

The authors declare no competing financial interest.

■ ACKNOWLEDGMENTS

W.-M.R. and T.-J.Y. acknowledge the support from the National Natural Science Foundation of China (NSFC, Grant Nos. 22101040 and 21722402). T.-J.Y. acknowledges the support from the China Postdoctoral Science Foundation (BX2021050 and 2021M690517). This work was supported by the Fundamental Research Funds for the Central Universities (DUT22LAB609).

■ REFERENCES

(1) Guo, T.; Li, Z.; Bi, L.; Fan, L.; Zhang, P. Recent advances in organic synthesis applying elemental selenium. *Tetrahedron* **2022**, *112*, 132752−132783.

(2) Menon, S.; Shrudhi Dev, K. S.; Santhiya, R.; Rajeshkumar, S.; Venkat Kumar, S. Selenium nanoparticles: A potent chemotherapeutic agent and an elucidation of its mechanism. *Colloids Surf., B* **2018**, *170*, 280−292.

(3) Zhu, M.; Niu, G.; Tang, J. Elemental Se: fundamentals and its optoelectronic applications. *J. Mater. Chem. C* **2019**, *7*, 2199−2206.

(4) Bhattacharya, A.; Turowski, S.; I Martin, D. S.; Rajput, A. Y.; Rustum, M. R.; Hoffman, M.; Seshadri, M. Magnetic resonance and fluorescence-protein imaging of the antiangiogenic and anti-tumor efficacy of selenium in an orthotopic model of human colon cancer. *Anticancer Res.* **2011**, *31*, 387−394.

(5) Sarma, B. K.; Mugesh, G. Glutathione peroxidase (GPx)-like antioxidant activity of the organoselenium drug ebselen: unexpected complications with thiol exchange reactions. *J. Am. Chem. Soc.* **2005**, *127*, 11477−11485.

(6) Eftekhari, A. The rise of lithium−selenium batteries. *Sustainable Energy Fuels* **2017**, *1*, 14−29.

(7) Jin, J.; Tian, X.; Srikanth, N.; Kong, L. B.; Zhou, K. Advances and challenges of nanostructured electrodes for Li−Se batteries. *J. Mater. Chem. A* **2017**, *5*, 10110−10126.

(8) Feng, R.; Wei, C.; Tu, S. The roles of selenium in protecting plants against abiotic stresses. *Environ. Exp. Bot.* **2013**, *87*, 58−68.

(9) Domokos-Szabolcsy, E.; Marton, L.; Sztrik, A.; Babka, B.; Prokisch, J.; Fari, M. Accumulation of red elemental selenium nanoparticles and their biological effects in Nicotinia tabacum. *Plant Growth Regul.* **2012**, *68*, 525−531.

(10) Parker, J. N.; Parker, P. M. *Selenium: A Medical Dictionary, Bibliography, and Annotated: Research Guide to Internet References* Icon Group International: San Diego, 2004.

(11) Liang, Y.; Lan, S.; Deng, P.; Zhou, D.; Guo, Z.; Chen, H.; Zhan, H. Regioregular and regioirregular poly(selenophene-perylene diimide) acceptors for polymer−polymer solar cells. *ACS Appl. Mater. Interfaces* **2018**, *10*, 32397−32403.

(12) Wu, X.; He, J.; Hu, R.; Tang, B. Z. Room-temperature metal-free multicomponent polymerizations of elemental selenium toward stable alicyclic poly(oxaselenolane)s with high refractive index. *J. Am. Chem. Soc.* **2021**, *143*, 15723−15731.

(13) Zhang, C.-J.; Hu, L.-F.; Yang, J.-L.; Cao, X.-H.; Zhang, X.-H. Alternating copolymerization of γ-selenobutyrolactone with episulfides for high refractive index selenium-containing polythioesters. *Eur. Polym. J.* **2020**, *133*, 109776−109781.

(14) Wu, X.; Lin, H.; Dai, F.; Hu, R.; Tang, B. Z. Functional Polyselenoureas for selective gold recovery prepared from catalyst-free multicomponent polymerizations of elemental selenium. *CCS Chem.* **2020**, *2*, 191−202.

(15) Ji, S.; Cao, W.; Yu, Y.; Xu, H. Visible-light-induced self-healing diselenide-containing polyurethane elastomer. *Adv. Mater.* **2015**, *27*, 7740−7745.

(16) Ma, N.; Li, Y.; Xu, H.; Wang, Z.; Zhang, X. Dual redox responsive assemblies formed from diselenide block copolymers. *J. Am. Chem. Soc.* **2010**, *132*, 442−443.

(17) Cao, W.; Zhang, X.; Miao, X.; Yang, Z.; Xu, H. γ-Ray responsive supramolecular hydrogel based on a diselenide-containing polymer and a peptide. *Angew. Chem., Int. Ed.* **2013**, *52*, 6233−6237.

(18) Zhao, P.; Xia, J.; Cao, M.; Xu, H. Wavelength-controlled light-responsive polymer vesicle based on Se−S dynamic chemistry. *ACS Macro Lett.* **2020**, *9*, 163−168.

(19) Perera, M. M.; Chimala, P.; Elhusain-Elnegres, A.; Heaton, P.; Ayres, N. Reversibly softening and stiffening organogels using a wavelength-controlled disulfide-diselenide exchange. *ACS Macro Lett.* **2020**, *9*, 1552−1557.

(20) Zhang, L.; Sun, C.; Tan, Y.; Xu, H. Selenium-sulfur-doped carbon dots with thioredoxin reductase activity. *CCS Chem.* **2022**, *4*, 2239−2248.

(21) Rowan, S. J.; Cantrill, S. J.; Cousins, G. R. L.; Sanders, J. K. M.; Stoddart, J. F. Dynamic covalent chemistry. *Angew. Chem., Int. Ed.* **2002**, *41*, 898−952.

(22) Corbett, P. T.; Leclaire, J.; Vial, L.; West, K. R.; Wietor, J. L.; Sanders, J. K. M.; Otto, S. Dynamic combinatorial chemistry. *Chem. Rev.* **2006**, *106*, 3652−3711.

(23) Lehn, J. M. Dynamic combinatorial chemistry and virtual combinatorial libraries. *Chem. - Eur. J.* **1999**, *5*, 2455−2463.

(24) Zou, W.; Dong, J.; Luo, Y.; Zhao, Q.; Xie, T. Dynamic Covalent Polymer Networks: from Old Chemistry to Modern Day Innovations. *Adv. Mater.* **2017**, *29*, 1606100−1606117.

(25) Minkenberg, C. B.; Florusse, L.; Eelkema, R.; Koper, G. J.; van Esch, J. H. Triggered self-assembly of simple dynamic covalent surfactants. *J. Am. Chem. Soc.* **2009**, *131*, 11274−11275.

(26) Minkenberg, C. B.; Li, F.; van Rijn, P.; Florusse, L.; Boekhoven, J.; Stuart, M. C. A. G.; Koper, J.; Eelkema, M. R.; van Esch, J. H. Responsive vesicles from dynamic covalent surfactants. *Angew. Chem., Int. Ed.* **2011**, *50*, 3421−3424.

(27) Jin, Y.; Yu, C.; Denman, R. J.; Zhang, W. Recent advances in dynamic covalent chemistry. *Chem. Soc. Rev.* **2013**, *42*, 6634−6654.

(28) Chakma, P.; Konkolewicz, D. Dynamic covalent bonds in polymeric materials. *Angew. Chem., Int. Ed.* **2019**, *58*, 9682−9695.

(29) Liu, C.; Tan, Y.; Xu, H. Functional polymer materials based on dynamic covalent chemistry. *Sci. China Mater.* **2022**, *65*, 2017−2034.

(30) Xia, J.; Tan, Y.; Xu, H. Selenium-containing dynamic covalent polymers. *Acta Polym. Sin.* **2020**, *51*, 1190−1200.

(31) Fan, F.; Ji, S.; Sun, C.; Liu, C.; Yu, Y.; Fu, Y.; Xu, H. Wavelength-controlled dynamic metathesis: a light-driven exchange reaction between disulfide and diselenide bonds. *Angew. Chem., Int. Ed.* **2018**, *57*, 16426−16430.

(32) Ma, Y.-T.; Liu, M.-C.; Zhou, Y.-B.; Wu, H.-Y. Synthesis of organoselenium compounds with elemental selenium. *Adv. Synth. Catal.* **2021**, *363*, 5386−5406.

(33) Wang, Y.; Zhang, W.-X.; Wang, Z.; Xi, Z. Procedure-controlled selective synthesis of 5-acyl-2-iminothiazolines and their selenium and tellurium derivatives by convergent tandem annulation. *Angew. Chem., Int. Ed.* **2011**, *50*, 8122−8126.

(34) Huang, M.-Q.; Li, T.-J.; Liu, J.-Q.; Shatskiy, A.; Kärkäs, M. D.; Wang, X.-S. Switchable copper-catalyzed approach to benzodithiole, benzothiaselenole, and dibenzodithiocine skeletons. *Org. Lett.* **2020**, *22*, 3454.

(35) Nakano, K.; Tatsumi, G.; Nozaki, K. Synthesis of sulfur-rich polymers: copolymerization of episulfide with carbon disulfide by using [PPN]Cl/(salph)Cr(III)Cl system. *J. Am. Chem. Soc.* **2007**, *129*, 15116−15117.

(36) Yue, T.-J.; Zhang, M.-C.; Gu, G.-G.; Wang, L.-Y.; Ren, W.-M.; Lu, X.-B. Precise synthesis of poly(thioester)s with diverse structures by copolymerization of cyclic thioanhydrides and episulfidesmediated by organic ammonium salts. *Angew. Chem., Int. Ed.* **2019**, *58*, 618−623.

(37) Zhu, X.-F.; Xie, R.; Yang, G.-W.; Lu, X.-Y.; Wu, G.-P. Precisely alternating copolymerization of episulfides and isothiocyanates: a practical route to construct sulfur-rich polymers. *ACS Macro Lett.* **2021**, *10*, 135−140.

(38) Chao, J.-Y.; Yue, T.-J.; Ren, B.-H.; Gu, G.-G.; Lu, X.-B.; Ren, W.-M. Controlled disassembly of elemental sulfur: an approach to the precise synthesis of polydisulfides. *Angew. Chem., Int. Ed.* **2022**, *61*, No. e202115950.

(39) The deviation of maximum absorbance wavelength of $CH_3SeSeCH_3$ and Se/MT copolymer can be attributed to the difference in specific structure and the phase effect of the polymer.

(40) A peak with m/z = 844.7879 was observed, and can be attributed to the species of $[C_{27}H_{30}O_3S_3Se_3 + Ag]^+$, of which the structure could be − $(PhOCH_2)CHCH_2SS{-}(PhOCH_2)CHCH_2SSe{-}(PhOCH_2)CHCH_2SeSe{-}$ or $[-(PhOCH_2)CHCH_2SSe-]_3$, suggesting the formation of S−S, and Se−Se bonds. the isotope of species analysis of this peak confirmed the structure of these fragments should be − $(PhOCH_2)CHCH_2SS{-}(PhOCH_2)CHCH_2SSe{-}(PhOCH_2)CHCH_2SeSe{-}$ (Figure S35).

(41) Mizen, M. B.; Wrighton, M. S. Reductive addition of CO_2 to 9,10-phenanthrenequinone. *J. Electrochem. Soc.* **1989**, *136*, 941−946.

(42) Gurkan, B.; Simeon, F.; Hatton, T. A. Quinone reduction in ionic liquids for electrochemical co_2 separation. *ACS Sustainable Chem. Eng.* **2015**, *3*, 1394−1405, DOI: 10.1021/acssuschemeng.5b00116.

(43) Apaydin, D. H.; Glowacki, E. D.; Portenkirchner, E.; Sariciftci, N. S. Direct electrochemical capture and release of carbon dioxide using an industrial organic pigment: quinacridone. *Angew. Chem., Int. Ed.* **2014**, *53*, 6819−6822.

(44) Singh, P.; Rheinhardt, J. H.; Olson, J. Z.; Tarakeshwar, P.; Mujica, V.; Buttry, D. A. Electrochemical capture and release of carbon dioxide using a disulfide-thiocarbonate redox cycle. *J. Am. Chem. Soc.* **2017**, *139*, 1033−1036.

https://doi.org/10.1021/acs.macromol.3c01628
Macromolecules 2024, 57, 1319−1327